



PERGAMON

Vision Research 42 (2002) 401–415

**Vision  
Research**[www.elsevier.com/locate/visres](http://www.elsevier.com/locate/visres)

# Functionally rodless mice: transgenic models for the investigation of cone function in retinal disease and therapy

A.L. Lyubarsky<sup>a</sup>, J. Lem<sup>b</sup>, J. Chen<sup>c</sup>, B. Falsini<sup>d</sup>, A. Iannaccone<sup>e</sup>, E.N. Pugh Jr.<sup>a,\*</sup><sup>a</sup> Department of Ophthalmology, F.M. Kirby Center for Molecular Ophthalmology, Stellar-Chance Building, Room 309B, School of Medicine, University of Pennsylvania, Philadelphia, PA 19104-6069, USA<sup>b</sup> Department of Ophthalmology, New England Medical Center, Boston, MA 02111-1533, USA<sup>c</sup> Department of Ophthalmology, University of Southern California, Los Angeles, CA 90033, USA<sup>d</sup> Department of Ophthalmology, Catholic University, Rome 168, Italy<sup>e</sup> Department of Ophthalmology, University of Tennessee, Memphis, TN 38163, USA

Received 14 May 2001; received in revised form 6 August 2001

## Abstract

Two genetically engineered strains of mice were used to characterize murine cone function electroretinographically, without interference of rod-driven responses: (1) mice with a deletion of the gene for the rod transducin  $\alpha$ -subunit (transducin  $\alpha$ -/-), and (2) mice with rod arrestin deleted (arrestin -/-). In the first three months of age, both strains have a normal complement of rods and normal rod structure, but transducin  $\alpha$ -/- mice have no rod-driven responses to light, while rod-driven activity of arrestin -/- mice can be suppressed by a single intense flash for hours. In response to intense flashes the electroretinograms of these strains of mice showed a readily identifiable, pure-cone a-wave of  $\sim 10$   $\mu$ V saturating amplitude. A 530 nm background that saturates rod responses of wild type mice was found to desensitize the b-wave responses of mice of both transgenic lines, whether the b-waves were driven by photons captured by M- or UV-cone pigments. The desensitizing effect of the 530 nm background on UV-pigment driven responses provides new evidence in support of the hypothesis of functional co-expression of the M-pigment in cones expressing primarily the UV-pigment. © 2002 Published by Elsevier Science Ltd.

**Keywords:** Phototransduction; Light adaptation; Transgenic mice; Transducin; Arrestin

## 1. Introduction

One goal of therapeutic intervention in human hereditary eye disease is the preservation of cone function. Since the mouse is the principal mammalian genetic model for the investigation of retinal disease and therapy, an important step toward evaluating interventions aimed at preserving cone viability is the development of methods of assessing murine cone function that are quantitative and noninvasive.

Electroretinographic analysis of the a-wave and scotopic b-wave have clearly met these criteria in the evaluation of rod function in mice. There is now an abundance of evidence that the a-wave of the electroretinogram (ERG) in rodents results primarily from

suppression of rod circulating current (Green & Kapousta-Bruneau, 1999; Hetling & Pepperberg, 1999; Lyubarsky & Pugh, 1996; Penn & Hagsins, 1972; reviewed in Pugh, Falsini, & Lyubarsky, 1998). Substantial evidence also supports the hypothesis that the primary current generator underlying the scotopic b-wave is the rod bipolar (Robson & Frishman, 1995, 1996; reviewed in Pugh et al., 1998). As a consequence, most features of the rod circulating current and rod bipolar responses can be monitored simply and non-invasively with the ERG, allowing ready evaluation of the effects of transgenic manipulations and therapeutic intervention on retinal rod function.

Electroretinographic assessment of murine cone-driven retinal activity has lagged substantially behind that of rod-driven activity. Among the reasons for the lag in the development of ERG-based assessment of cone activity are difficulties posed by the relatively small magnitude of the cone-driven ERG components, by the

\* Corresponding author. Tel.: +1-215-898-2403; fax: +1-215-573-7155.

E-mail address: [pugh@mail.med.upenn.edu](mailto:pugh@mail.med.upenn.edu) (E.N. Pugh Jr.).

spectral characteristics of the murine cone pigments, and by the relative insensitivity of cone-driven responses, as now explained.

Rods are the predominant class of photoreceptors in mice, with cones constituting only about 3% of the total complement of receptors (Carter-Dawson & LaVail, 1979a,b). An electrical consequence of rod numerical predominance is that the suppression of cone circulating current per se can in principle only generate only a very small field potential relative to that of rods, and thus, the cone a-wave has been very difficult to distinguish incontrovertibly from the rod a-wave and then, to effectively characterize.

The spectral characteristics of murine cones further complicate the task of isolating and characterizing mouse cone-driven ERG responses, especially the cone a-wave. One of the two murine cone pigments has its  $\lambda_{\max}$  at 508 nm (Sun, Macke, & Nathans, 1997), close to that of rhodopsin ( $\lambda_{\max} = 498$  nm), making it very difficult to discriminate rod- and cone-driven activity by a Purkinje shift. In addition, the other murine cone pigment, namely that belonging to the same family as the human S-cone pigment, has its peak in the UV ( $\lambda_{\max} = 359$  nm) (Yokoyama, Radlwimmer, & Kawamura, 1998), so that UV light as well as calibration equipment not normally used for human ERG apparatuses is needed for quantifying and delivering stimuli appropriate to characterizing murine UV-cones. Yet another complicating spectral characteristic of murine cones is the co-expression of both UV- and M-pigments in individual cone cells (Applebury et al., 2000; Gloesman & Ahnelt, 1998; Rohlich, van Veen, & Szel, 1994).

The standard method of isolating cone-driven ERG responses from those of rods is to expose the retina to a rod-saturating background, that is, to a light stimulus that completely suppresses the rod circulating current. While necessary in the investigation of normal mice, use of a rod-saturating backgrounds adds to the aforementioned list of difficulties in characterizing murine cone-driven responses, since it cannot be assumed a priori that exposure to a background does not lead to modification of the functional characteristics of the cone-driven responses.

For the reasons just summarized—the relatively small magnitude of murine cone-driven responses, the potentially confusing spectral characteristics of murine cones, and the problem of cone adaptation by rod-saturating backgrounds it—would be valuable to be able to characterize murine cone-driven ERGs responses under conditions that absolutely exclude all rod-driven activity. We thus undertook an investigation of cone-driven ERGs in mice with genetic modifications that cause all rod-driven responses to be either completely absent, or readily inactivated by stimuli that cause no lasting activation of cones. Such animals may be called “stationary functionally rodless mice”.

In this investigation we describe the cone-driven responses of two types of functionally rodless mice. The first, transducin  $\alpha-/-$ , lacks the alpha-subunit of the rod transducin; this genotype results in complete inactivation of the rod phototransduction cascade (Calvert et al., 2000). The second, arrestin  $-/-$ , has the rod arrestin gene inactivated; this genetic modification leaves the activation phase of rod phototransduction intact, but causes a profound retardation in the recovery of rods to illumination (Xu et al., 1997).

## 2. Methods

### 2.1. Animal maintenance and light regimen

All experimental procedures were performed in compliance with National Institute of Health guidelines, as approved by the University of Pennsylvania Animal Care and Use Committee. Animals used in this study were transducin  $\alpha-/-$  and arrestin  $-/-$  mice described previously (Calvert et al., 2000; Chen, Simon, Matthes, Yasumura, & LaVail, 1999; Xu et al., 1997). Both types of transgenic animals had 129SV background. Wild type 129SV mice were obtained from Jackson Laboratories (Bar Harbor, Maine). All animals were maintained on a 12 h 2.5 lux light/dark cycle as described in Pugh et al. (1998), and were dark-adapted overnight for at least 12 h before the experiment.

### 2.2. Histology

Retinal histology of the two strains of transgenic mice employed in the present investigation has been reported previously (Calvert et al., 2000; Chen et al., 1999; Xu et al., 1997). At the ages (6–8 weeks) of the mice whose ERGs are presented here, both strains have outer nuclear layer and outer segment layer thicknesses that are indistinguishable from those of wild type, providing the animals are reared under low to moderate illumination, as was the case. Older mice of the arrestin  $-/-$  genotype exhibit thinning of the ONL at later stages, especially if reared under higher intensity illumination (Chen et al., 1999).

### 2.3. Electroretinogram recordings

The methods of ERG recording have been described in detail previously (Lyubarsky, Falsini, Pennesi, Valentini, & Pugh, 1999). In brief, ERGs were recorded from anesthetized mice with a differential amplifier with bandwidth 0.1 Hz to 1 kHz, and sampled and digitized at 5 kHz. The corneal electrode was a platinum wire, while the reference electrode was a tungsten needle inserted subcutaneously in the forehead. The recording chamber served dually as a Faraday cage and a ganzfeld,

with ports and baffles for illumination. Preparation of the mice for recordings were performed under dim red light. Before recording commenced, animals were maintained in complete darkness for 15 min.

#### 2.4. Light stimulation and calibration

The methods for light stimulation and calibration of light stimuli have been given in detail in Lyubarsky et al. (1999). Flash intensities, background intensities and derived parameters such as flash sensitivity will be reported in units of photons  $\mu\text{m}^{-2}$  or photons  $\mu\text{m}^{-2}\text{s}^{-1}$  at the cornea; these numbers represent the flux density incident upon a photodiode positioned at the location of the mouse's eye in the ganzfeld stimulator. We also identify some stimuli in terms of their computed efficacy in isomerizing the UV- and M-cone pigments. The estimation of the end-on collecting area  $a_{\text{cone}}$  of murine cones at the retina for light at the pigment  $\lambda_{\text{max}}$  is given in Lyubarsky et al. (1999), and we adopt the same value,  $a_{\text{cone}}(\lambda_{\text{max}}) = 2.4 \mu\text{m}^2$ .

The calculation of the fractional isomerization ( $f_{\text{isom}}$ ) or “bleached fraction” of cone pigment generated by a specific stimulus (monochromatic or broadband) is given in Lyubarsky, Chen, Simon, and Pugh (2000, Eqs. (5) & (6)). In keeping with our previous analysis, we will assume that each murine cone contains  $N_{\text{tot}} = 3.5 \times 10^7$  molecules of visual pigment, though not all of the same  $\lambda_{\text{max}}$ , as explained further below.

It will be useful to relate stimulus flux densities measured radiometrically at the plane of the mouse cornea to photometric units. Specifically, given that the mouse is situated in a homogeneous, isotropic ganzfeld, the relationship between the scotopic luminance of the ganzfeld wall and the photon flux density (PFD) measured at the plane of the cornea can be expressed as follows:<sup>1</sup>

$$\text{PFD} = \pi L'_v \times 1.5 \times 10^{15}, \quad (1)$$

where the units of each quantity in Eq. (1) are PFD (photons  $\text{m}^{-2}\text{s}^{-1}$ ,  $\lambda = 507 \text{ nm}$ ),  $\pi$  (sr),  $L'_v$  ( $\text{lm sr}^{-1}\text{m}^{-2}$ ),  $1.5 \times 10^{15}$  (photons  $\text{s}^{-1}\text{lm}^{-1}$ ) (conversion factor) and where all photometric units are scotopic, and “photons” have the wavelength 507 nm in a vacuum. Note that an equivalent definition of the unit of  $L'_v$  is  $\text{cd m}^{-2}$ , since by definition,  $1 \text{ cd} \equiv 1 \text{ lm sr}^{-1}$ , and also that the photon flux density in Eq. (1) must be expressed per  $\text{m}^2$  for consistency of unit magnitudes across the equation (though we report flux densities in photons  $\mu\text{m}^{-2}$ ).

<sup>1</sup> An expression closely related to Eq. (1) was given in Pennesi, Lyubarsky, and Pugh (1998), where the incorrect factor  $2\pi$  rather than the correct factor  $\pi$  was used. A derivation of the correct relationship and the conversion factors involved can be found in Wyszecki and Stiles (1982, Chap. 4). We thank John Robson for pointing out this mistake to us.

#### 2.5. Analysis of the activation phase of the cone a-wave: the pigment co-expression problem

Substantial histological evidence has been published that most murine cones express both cone visual pigments (Applebury et al., 2000; Gloesman & Ahnelt, 1998), and electrophysiological evidence consistent with such co-expression has been presented (Lyubarsky et al., 1999). Cone pigment co-expression presents a novel problem for application of the analysis of the activation phase of the cascade developed by Lamb and Pugh (1992) to murine cone a-waves. Here we develop and apply a simplified analysis which neglects retinotopic variation in the co-expression in UV-cones (Applebury et al., 2000). Specifically, we will assume that there are only two cone classes, one expressing predominantly the cone pigment with  $\lambda_{\text{max}} = 359 \text{ nm}$  (UV-cones), and the second expressing predominantly the cone pigment with  $\lambda_{\text{max}} = 508 \text{ nm}$  (M-cones). Given the total complement  $N_{\text{tot}}$  of pigment molecules per cone to be fixed, we assume a minor proportion of co-expressed cone pigment of the second type. In this framework, cone pigment co-expression is characterized by two proportionality parameters,  $p_{\text{UV} \rightarrow \text{M}}$  (proportion of UV-pigment in the total complement  $N_{\text{tot}}$  of pigment molecules of the M-cones) and  $p_{\text{M} \rightarrow \text{UV}}$  (proportion of M-pigment in the total complement  $N_{\text{tot}}$  of pigment molecules of the UV-cones). With these definitions and assumptions it follows that the number  $\Phi$  of photoisomerized pigment molecules produced in a “UV-cone” by a flash that isomerizes a fraction  $f_{\text{UV}}$  of the UV-pigment and a fraction  $f_{\text{M}}$  of the M-pigment will be given by

$$\Phi = [f_{\text{UV}}(1 - p_{\text{M} \rightarrow \text{UV}}) + f_{\text{M}}p_{\text{M} \rightarrow \text{UV}}]N_{\text{tot}}. \quad (2)$$

This expression is useful because the fractions  $f_{\text{UV}}$  and  $f_{\text{M}}$  can be computed from knowledge of the flash spectrum and intensity regardless of how the pigment is disposed (see Lyubarsky et al., 2000), leaving only a single parameter, the co-expression proportion  $p_{\text{M} \rightarrow \text{UV}}$  to be specified or estimated. An expression similar to Eq. (2) can readily be derived for estimating the total number of photoisomerizations in the “M-cones” produced by a specific flash.

The model of the activation phase of the photo-transduction cascade developed by Lamb and Pugh (1992) and Pugh and Lamb (1993) predicts that in response to a flash producing  $\Phi$  photoisomerizations in a photoreceptor,  $F$ , the fractional cGMP-activated current, will decline as

$$F(t) = \exp[-(1/2)\Phi A(t - t_{\text{delay}})^2]. \quad (3)$$

The parameter,  $A$ , the “amplification constant,” embodies the combined gain factors of the several stages of the transduction cascade and can be expressed as

$$A = v_{\text{G}}c_{\text{GE}}\beta_{\text{sub}}n_{\text{chan}}, \quad (4)$$

where  $v_G$  is the rate with which a single activated pigment molecule generates active G-proteins,  $c_{GE}$  is the coupling efficiency between the G-protein and the effector enzyme, phosphodiesterase (*PDE*),  $\beta_{\text{sub}}$  is the rate constant of hydrolysis of a single catalytic subunit of the *PDE*, and  $n_{\text{chan}}$  is the Hill coefficient of the cGMP-activated channel. (See Leskov et al. (2000) for a recent analysis and summary of the factors contributing to amplification in rods.)

## 2.6. Parameters characterizing the cone-wave activation phase

One goal of this work was to develop the groundwork for application of the activation model (Eq. (3)), to cone-driven a-waves from functionally rodless mice. To achieve this goal, several parameters need to be specified or estimated. We now examine this matter.

*Pigment co-expression proportions:* Application of the model requires estimation of the number of photoisomerizations per cone per flash, a number affected by cone pigment co-expression (Eq. (2)). The analysis of Applebury et al. (2000) indicates that about 20% or so of the total retina (the dorsal-most region) of the mouse has cones that express only the M-pigment, and that everywhere else the retina is dominated by cones that seem to express primarily the UV-pigment, but co-express the M-pigment. In our simplified “two-cone class” framework we accordingly assume that  $p_{UV \rightarrow M} = 0$ , i.e., that the M-cones do not co-express any UV-pigment, and let the proportion of M-pigment expressed in UV-cones,  $p_{M \rightarrow UV}$ , be an unknown, to be constrained or estimated from the data.

*The amplification constant:* Only a single cone-specific G-protein, GNAT2, has been identified (GenBank, NM\_008141) and only one cone-specific *PDE* is known, and only a single cone-specific cGMP-activated channel (Biel et al., 1999; GenBank, AJ243933). Thus, it can tentatively be assumed that amongst mouse cones the only difference in the effect on the activation phase of the cascade of an isomerized UV-pigment molecule, and that of an isomerized M-pigment, lies in the rate,  $v_{UV,G}$  or  $v_{M,G}$ , with which the particular isomerized molecule activates copies of the one type of G-protein, GNAT2. It follows that only two amplification coefficients,  $A_{UV}$  and  $A_M$  one for each type of pigment need be specified. Because there is no evidence indicating at this time that the rates  $v_{UV,G}$  or  $v_{M,G}$  differ, we will adopt the working assumption that  $A_{UV} = A_M$  and hereafter simply use  $A$  to refer to this parameter. In summary, given that mouse cones have only a single G-protein and a single *PDE*, the assumption  $A_{UV} = A_M$  is equivalent to the assumption that a photoactivated cone pigment molecule of either type activates the one cone-specific G-protein at the same rate. (If the G-protein rates  $v_{UV,G}$  or  $v_{M,G}$  turn out to be different, then Eq. (2) can be appropriately modified,

but at this time such complexity in analysis is unwarranted.)

*Saturating amplitude of the cone a-wave:* In application of Eq. (2) to rod ERGs, the assumption is made that that  $a_{\text{max}}$ , the saturating amplitude of the a-wave, corresponds to the complete suppression of the rod circulating current, so that in Eq. (2),  $F(t) = [1 - a(t)/a_{\text{max}}]$ ; this assumption is well supported (Lyubarsky & Pugh, 1996; Pugh et al., 1998). The corresponding assumption to be made here is that  $a_{\text{max}}$  of the functionally rodless animals represents complete suppression of the circulating current of both classes of cones, having respective saturating a-wave amplitudes  $a_{\text{max,UV}}$  and  $a_{\text{max,M}}$  with the constraint that  $a_{\text{max}} = a_{\text{max,UV}} + a_{\text{max,M}}$ . To apply Eq. (3),  $a_{\text{max,UV}}$  and  $a_{\text{max,M}}$  need to be determined. Given the constraint, however, it suffices to determine the ratio of the amplitudes,  $a_{\text{max,UV}}/a_{\text{max,M}}$ . Here we will assume that  $a_{\text{max,UV}}/a_{\text{max,M}} = 4$ , estimated from the ratio of cone b-wave sensitivities at 360 and 510 nm (Lyubarsky et al., 1999, 2000). This sensitivity ratio should reflect the cone ratio, assuming that the cone b-wave represents primarily the cone on-bipolar responses, and that there is an invariant numerical correspondence between cones and their on-bipolars throughout the retina. Applebury et al. (2000) report a 3:1 ratio for the total mRNA of the UV-cone pigment and the M-cone pigment in the mouse retina. This ratio should underestimate the ratio of the cone types because the total M-pigment mRNA includes that due to the co-expression of M-pigment in UV-cones, i.e., in the cones expressing primarily the UV-pigment. Thus, Applebury et al.’s mRNA data are consistent with a UV-cone/M-cone ratio of about 4. (In Table 1 of this paper the average b-wave sensitivity ratio for the transducin  $\alpha$ -/- mice is 2.1, and 3.6 for the arrestin -/- mice, but given the interanimal variability and extensive previous work on wild type mice, we adopt the latter value.) Given  $a_{\text{max,UV}}/a_{\text{max,M}} = 4$ , and the electrical constraint  $a_{\text{max,UV}} + a_{\text{max,M}} = a_{\text{max}}$ , where  $a_{\text{max}}$  is the observed saturating cone a-wave amplitude, it follows that the saturating amplitudes  $a_{\text{max,UV}}$  and  $a_{\text{max,M}}$  of the two cone populations are determined once  $a_{\text{max}}$  is measured.

*Cone membrane time constant:* We used Eq. (3) in the analysis of the activation phase of the cone-driven a-waves, applying the modification developed by Smith and Lamb (1997), which explicitly convolves Eq. (3) with the membrane time constant,  $\tau_{\text{mem}}$ . Based on their analysis of human cone a-waves, and that of other investigators (Cideciyan & Jacobson, 1996), we anticipate  $\tau_{\text{mem}} \approx 5$  ms.

## 2.7. Measurements of the spectral sensitivity of the cone-driven b-wave

As shown previously, low-pass filtered cone-driven b-wave responses of wild type mice for flashes of intensities that elicit responses  $\leq 30\%$  of the saturating am-

Table 1  
Parameters of cone-driven ERGs of wild type and functionally rodless mice

Parameter	Wild type	Transducin $\alpha$ -/-		Arrestin -/-	
	Standard background	Standard background	No background	Standard background	No background
Saturating cone a-wave ( $\mu\text{V}$ )	–	–	$10 \pm 6$	–	$8.8 \pm 1.5$
$N$	–	–	9	–	5
Saturating cone b-wave ( $\mu\text{V}$ )	$100 \pm 36$	–	$120 \pm 31$	–	$130 \pm 17$
$N$	11	–	9	–	7
Abs. sensitivity, 361 nm ( $\text{nV photon}^{-1} \mu\text{m}^2$ )	$18 \pm 13$	$12 \pm 5$	$15 \pm 6$	$23 \pm 4$	$61 \pm 42$
$N$	6	5	8	4	6
Abs. sensitivity, 513 nm ( $\text{nV photon}^{-1} \mu\text{m}^2$ )	$4.1 \pm 3.6$	$3.6 \pm 1.4$	$7.1 \pm 2.8$	$9.0 \pm 2.6$	$17 \pm 12$
$N$	6	5	9	4	8
Fract. sensitivity, 361 nm ( $\text{photon}^{-1} \mu\text{m}^2$ )	$(1.7 \pm 1.2) \times 10^{-4}$	$(1.2 \pm 0.3) \times 10^{-4}$	$(1.9 \pm 1.1) \times 10^{-4}$	$(2.0 \pm 0.4) \times 10^{-4}$	$(4.9 \pm 2.9) \times 10^{-4}$
$N$	6	5	8	4	8
Fract. sensitivity, 513 nm ( $\text{photon}^{-1} \mu\text{m}^2$ )	$(3.0 \pm 2.0) \times 10^{-5}$	$(3.4 \pm 0.9) \times 10^{-5}$	$(6.8 \pm 2.5) \times 10^{-5}$	$(7.9 \pm 1.8) \times 10^{-5}$	$(1.4 \pm 0.8) \times 10^{-4}$
$N$	6	5	9	4	8

Each pair of rows presents a parameter extracted from a sample of animals of the specified genotype and the number  $N$  of animals in the sample. The cone a-wave amplitude was extracted from experiments such as presented in Fig. 2, and has not been corrected for possible truncation by the b-wave. The cone b-wave amplitude was obtained from Gaussian-filtered traces, as in Fig. 3. Absolute and fractional sensitivities were determined for each animal individually, as illustrated in Fig. 3; see also Eqs. (2) and (3). The error terms given in the table are standard deviations.

plitude are linear in flash intensity (Lyubarsky et al., 1999). Such linearity can be expressed as follows:

$$B(t) = Q(\lambda)s_{\lambda}b(t), \quad (5)$$

where,  $B(t)$  is the low-pass filtered cone b-wave elicited by a monochromatic flash of wavelength  $\lambda$  and intensity  $Q(\lambda)$  photons  $\mu\text{m}^{-2}$ ,  $s_{\lambda}$  is the absolute sensitivity and  $b(t)$  is a dimensionless “dim-flash” response waveform having unity amplitude at its peak. In practice, in order to determine  $s_{\lambda}$  we measured the peak amplitude  $B_{\text{peak}} = B(t_{\text{peak}})$  of the filtered response (cf. Fig. 3); thus, from Eq. (5) with  $b(t_{\text{peak}}) = 1$  we obtain,

$$s_{\lambda} = B_{\text{peak}}/Q(\lambda). \quad (6)$$

Another useful quantity is the *fractional sensitivity*,  $S_{\lambda}$ , defined as

$$S_{\lambda} = (B_{\text{peak}}/B_{\text{peak,sat}})[1/Q(\lambda)] = s_{\lambda}/B_{\text{peak,sat}}, \quad (7)$$

where  $B_{\text{peak,sat}}$  is the amplitude of the saturated cone b-wave elicited by an intense achromatic flash. The fractional sensitivity specifies the fraction of the saturated response that is generated per unit of intensity, and is a useful measure for reducing variability between animals caused by variation in the absolute magnitudes of the saturating responses. Such variation may result from factors that are difficult to control precisely, such as

reference electrode placement and variation in the size of the mouse eye.

## 2.8. Definition of rod saturating background

A goal of this investigation was to determine to what extent the functional characteristics of nominally cone-driven ERG responses in normal mice are affected by the steady background of light used for isolating cone signals from those of rods. Two general problems that must be faced in the effort to reach this goal should be distinguished: (1) the intrusion of residual rod-driven signals under “cone-isolation” conditions; and (2) the effect of the cone-isolating background on the cone-driven responses. Thus, a background of steady light used to isolate cone-driven responses may be inadequately intense to completely suppress rod signals on the one hand, and/or be such as to diminish the sensitivity of the cone-driven responses.

The first problem can be characterized quantitatively in terms of the rod circulating current remaining in the presence of a steady background of a given intensity. It has been shown for a number of mammalian species that the suppression of the rod circulating current  $J_{\text{circ}}$  caused by steady illumination producing  $\phi$  photoisomerizations  $\text{rod}^{-1} \text{s}^{-1}$  is well described with the hyperbolic saturation relation

$$\frac{J_{\text{circ,dark}} - J_{\text{circ}}(\varphi)}{J_{\text{circ,dark}}} = \frac{\varphi}{\varphi + \varphi_{1/2}} \quad (8)$$

with  $\varphi_{1/2} = 150\text{--}300$  (Nakatani, Tamura, & Yau, 1991; Xu et al., 1997). The same formulation has been shown to apply to human rods, when the magnitude of the rod circulating current is estimated with the saturating a-wave amplitude (Thomas & Lamb, 1999), and to murine rods (Lyubarsky et al., 1999).

Assuming that Eq. (8) is strictly correct, no finite intensity steady background will *completely* suppress the rod circulating current, and thus the choice of a “rod-saturating” background intensity is determined by the acceptable level of the rod activity. In the present investigation we chose as the intensity of our standard rod-saturating background a 540 nm light that generates 31 000 photons  $\mu\text{m}^{-2}\text{s}^{-1}$  at the cornea. Assuming that for a mouse in a ganzfeld the end-on collecting area of a rod at the cornea is  $0.2 \mu\text{m}^2$  at 498 nm (Lyubarsky & Pugh, 1996), and that the luminous efficiency for rods at 540 nm is 0.65 (Wyszecki & Stiles, 1982), this background produces  $31\,000 \times 0.2 \times 0.65 \cong 4000$  photoisomerizations  $\text{rod}^{-1}\text{s}^{-1}$ . Furthermore, Eq. (8) with  $\varphi_{1/2} = 250$  (Lyubarsky et al., 1999), predicts that the standard background will suppress 94% of the rod cir-

culating current. These estimates are in general in line with previous estimates of the intensity of a rod-saturating backgrounds, 2000–6000 photoisomerizations  $\text{rod}^{-1}\text{s}^{-1}$ , reported for rods of various monkey (Tamura, Nakatani, & Yau, 1991), and for those of rabbit, cat, rat and cattle (Nakatani et al., 1991) obtained in suction electrode recordings. In some of the experiments reported here we have employed backgrounds somewhat more intense than the standard.

### 3. Results

#### 3.1. ERGs of transducin $\alpha$ -/- and arrestin -/- mice obtained in response to an intense flash

Fig. 1 compares ERGs of transducin  $\alpha$ -/- and arrestin -/- mice obtained in response to an intense flash with those of a wild type mouse obtained under three conditions: row *a*, dark adapted; row *b*, following a period of recovery in darkness after the initial flash; row *c*, in the presence of steady background. Record *a* from the wild type mouse illustrates well known features of the dark-adapted murine ERG: an initial corneal-negative component (highlighted in gray,  $-220 \mu\text{V}$

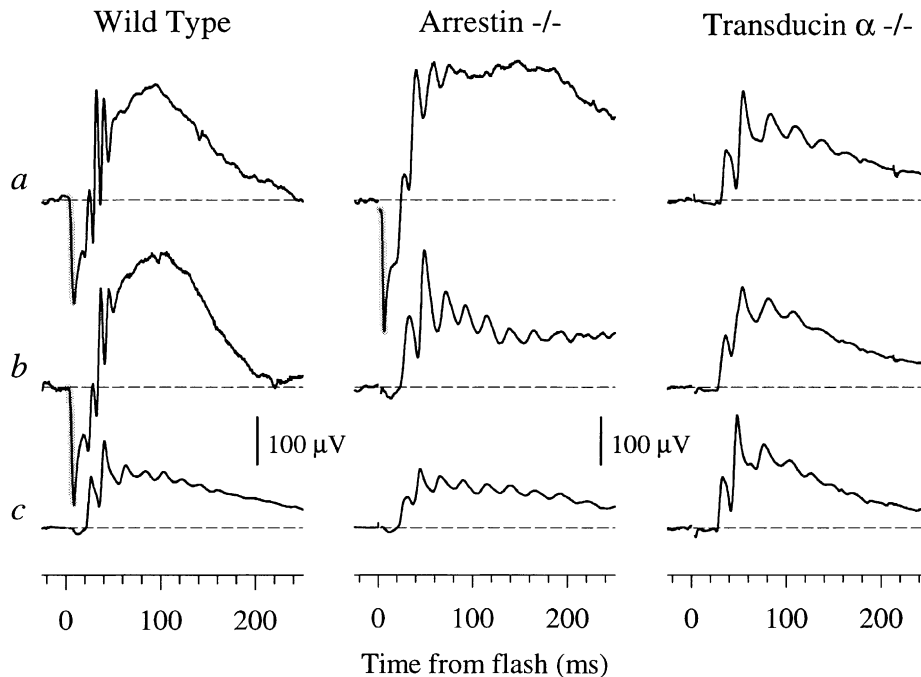


Fig. 1. ERGs of wild type, arrestin -/- and transducin  $\alpha$ -/- mice. All traces were obtained in response to the same flash, estimated to produce 530000 photoisomerizations  $\text{rod}^{-1}$ , but delivered to different animals (columns) and in different conditions (rows). Row *a* shows the response in the dark-adapted state. Row *b* shows the response to the same flash as in row *a*, delivered after an interval of darkness, whose duration was 2 min (wild type), 20 min (arrestin -/-) and 2 min (transducin  $\alpha$ -/-). Row *c* shows the response to the same flash as in rows *a*, *b*, but presented in the presence of a steady, 540 nm background estimated to produce 5900 photoisomerizations  $\text{rod}^{-1}\text{s}^{-1}$ . The responses of the wild type mouse, and those of the arrestin -/- mouse in rows *a* and *b* are single records, while all other traces shown are the averages of five records, recorded at 2 min intervals. The a-waves of wild type and arrestin -/- mice are highlighted in gray. (A 3.5 ms segment of some of the traces containing the flash artifact has been omitted from some traces for clarity.)

amplitude), the a-wave, followed by a larger positive-going b-wave (+450  $\mu\text{V}$ ) with superimposed oscillatory potentials. The ERG of the dark-adapted arrestin  $-/-$  mouse exhibits features very similar to that of the wild type mouse, though both a-wave and b-wave are about 20% larger, while the dark-adapted transducin  $\alpha-/-$  has no discernable a-wave, and a b-wave with much reduced amplitude. The absence of the a-wave in the dark-adapted transducin  $\alpha-/-$  mouse is consistent with the view that the a-wave originates primarily in the suppression of rod circulating current, since isolated rods of these mice have no rod responses (Calvert et al., 2000), and with the conclusion that the ERG is purely cone-driven.

The ERG of the wild type mouse recovers completely to its dark-adapted state in 2 min (row *b*), whereas that of the arrestin  $-/-$  mouse shows only a very small a-wave after 20 min of recovery. The extremely prolonged recovery of the a-wave arrestin  $-/-$  is expected from the essential requirement for arrestin to inactivate photoactivated rhodopsin (Xu et al., 1997). In similar experiments we found that the a-wave in the arrestin  $-/-$  mice exhibits little recovery even after up to 1 h dark adaptation, though its amplitude exhibits complete

recovery if the mice are retested two weeks later. Comparison of the traces obtained from the arrestin  $-/-$  and transducin  $\alpha-/-$  in row *b* of Fig. 1 supports the view that the ERG of the arrestin  $-/-$  mouse is purely cone-driven for at least 20 min after the exposure to the initial intense flash.

The third row of traces in Fig. 1, row *c*, presents responses to the same intense flash as was used to obtain the traces in rows *a*, *b*, but now delivered in the presence of a steady background estimated to produce 5900 photoisomerizations  $\text{rod}^{-1} \text{s}^{-1}$ . In this condition, the responses of wild type, arrestin  $-/-$  and transducin  $\alpha-/-$  mice are similar in form, and only a very small a-wave can be observed. Given that the transducin  $\alpha-/-$  mice have no rod phototransduction, and that rod responsiveness in arrestin  $-/-$  mice must be completely suppressed by a background of this intensity (Xu et al., 1997), it can be concluded that this small a-wave component originates exclusively in cone-driven neurons.

### 3.2. Cone a-waves of functionally rodless mice

Further analysis of the cone a-wave is presented in Fig. 2, where both time and amplitude scales have been

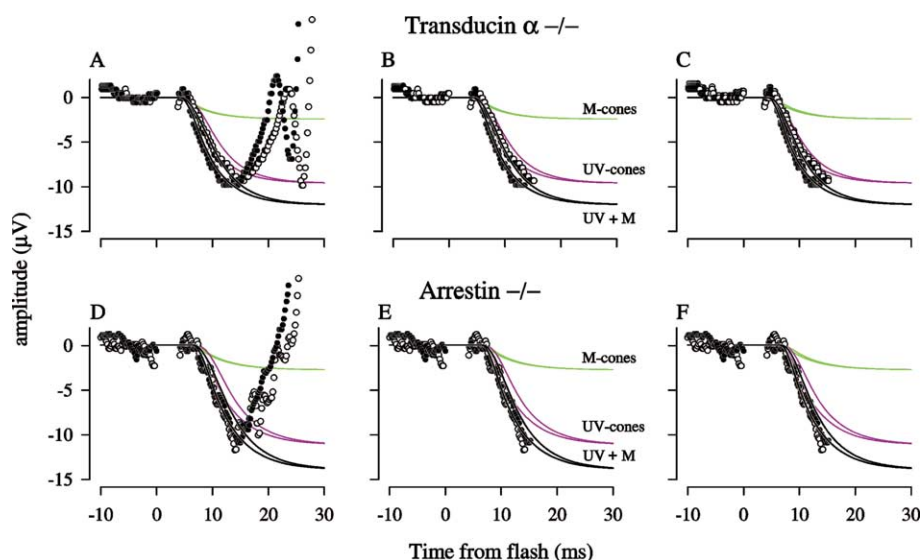


Fig. 2. Cone a-waves of a transducin  $\alpha-/-$  mouse and an arrestin  $-/-$  mouse in response to two intense flashes. Panels A–C repeat one pair of ERG traces (circles) obtained from a transducin  $\alpha-/-$  mouse, with three different sets of theory traces (lines); panels D–F repeat a pair of ERG traces (circles) from an arrestin  $-/-$  mouse, again with three different sets of theory traces (lines). The less intense of the pair of flashes was estimated to isomerize 0.4% of the M-cone pigment and 0.03% of the UV-cone pigment (white circles) while the more intense flash isomerized 1.2% of the M-cone pigment, and 0.09% of the UV-cone pigment, respectively (black circles). In panels A and D the complete ERG records over the time epoch are illustrated, while in panels B–D, F the ERG records have been truncated at the point of b-wave intrusion, approximately 15 ms after the flash. The recording bandwidth was 0.1–1000 Hz, and the sampling rate was 5000 Hz. Each trace shown is the average of at least 10 individual records, with the flashes delivered at 20 s intervals. (A 3.5 ms segment of the traces containing the flash artifact has been omitted for clarity.) The theoretical traces were computed with the formula of Smith and Lamb (1997), as explained in Section 2, with the following parameters. For all traces:  $a_{\text{max,UV}}/a_{\text{max,M}} = 4$ . For the traces in A–C:  $a_{\text{max}} = -12 \mu\text{V}$ ,  $t_{\text{delay}} = 2.8 \text{ ms}$ ,  $\tau_{\text{mem}} = 4.5 \text{ ms}$ ; for the traces in D–F:  $a_{\text{max}} = -14 \mu\text{V}$ ,  $t_{\text{delay}} = 5 \text{ ms}$ ,  $\tau_{\text{mem}} = 5 \text{ ms}$ . For panels A, D:  $A = 12.5 \text{ s}^{-2}$ ;  $p_{\text{M} \rightarrow \text{UV}} = 0$ . For B, E:  $A = 10 \text{ s}^{-2}$ ;  $p_{\text{M} \rightarrow \text{UV}} = 0.05$ . For C, F:  $A = 5 \text{ s}^{-2}$ ;  $p_{\text{M} \rightarrow \text{UV}} = 0.2$ . (“ $p_{\text{M} \rightarrow \text{UV}}$ ” is the proportion of M-pigment in the total pigment complement of the UV-cones.) In each panel A–F the green traces plot the predicted time course of the responses of the M-cones to the two flashes, the purple traces plot the predicted responses of the UV-cones, and the black traces plot the sum of the responses of the two classes of cones.

expanded about 10-fold relative to those used in Fig. 1. Fig. 2, panels A, D presents the responses of a transducin  $\alpha$ -/- and an arrestin -/- mouse to two intense flashes (circles), the more intense of which isomerized three times as much of the UV- and M-cone pigments as was isomerized by the less intense flash. The amplitudes of the cone a-waves of both arrestin -/- and transducin  $\alpha$ -/- mice are seen to be *saturated*: thus, increasing the flash intensity 3-fold caused a slight leftward shift of the responses in both mice, but did not increase the amplitude. The saturating amplitude of the cone a-wave of both mice is close to 10  $\mu$ V. A distinguishing kinetic feature of the cone a-waves is the relatively slow time to maximum, about 15 ms; in contrast, the rod a-wave obtained in response to such intense flashes (e.g., Fig. 3) invariably reaches its maximum in less than 10 ms (Lyubarsky et al., 1999, Fig. 2). Table 1 summarizes the saturated amplitudes of cone a-waves obtained in this manner from the two strains of functionally rodless mice.

We fitted the cone a-waves with a model of the activation phase of the phototransduction cascade, modified to include explicitly the cone membrane constant (Section 2; Cideciyan & Jacobson, 1996; Smith & Lamb, 1997). As seen in Fig. 2, a reasonable description of the a-wave data (black traces) can be obtained with  $\tau_{\text{mem}} \approx 5$  ms; this is close to the value,  $\tau_{\text{mem}} = 4.4 \pm 0.9$  ms, used by Smith and Lamb to describe human cone a-waves, and not dependent on other model parameters.

The amplification constant of the two hypothetical cone classes cannot be estimated independently of  $p_{M \rightarrow UV}$ , the proportion of M-pigment co-expressed in the UV-cones, as it was possible to describe the traces with  $A$  ranging from 12.5 to 5  $s^{-2}$ , providing that  $p_{M \rightarrow UV}$  varied correspondingly. Thus, the model with  $A = 12.5 s^{-2}$  gives a reasonable description of the a-waves of both transducin  $\alpha$ -/- and arrestin -/- mice in the limiting case  $p_{M \rightarrow UV} = 0$  (Fig. 2, panels A, D), but equally good descriptions were obtained with  $A = 10 s^{-2}$  and  $p_{M \rightarrow UV} = 0.05$  (panels B, D), and with  $A = 5 s^{-2}$  and  $p_{M \rightarrow UV} = 0.2$  (panels C, F). Co-expression proportions higher than 0.2 yielded theory traces that were materially poorer in fitting the data.

### 3.3. Sensitivity of the UV- and M-cone driven b-waves of transducin $\alpha$ -/- and arrestin -/- mice

The cone-driven b-wave of wild type mice has spectral sensitivity maxima near 360 and 510 nm (Lyubarsky et al., 1999), and so we measured the sensitivity of the cone b-wave responses of the transgenic mice for flashes of wavelength near these spectral maxima. Fig. 3 illustrates the way in the sensitivities were derived. Families of responses (black traces) were elicited by series of 362 nm (A) and 513 nm (B) flashes. The responses were low-pass filtered to obtain the thickened gray lines, and the

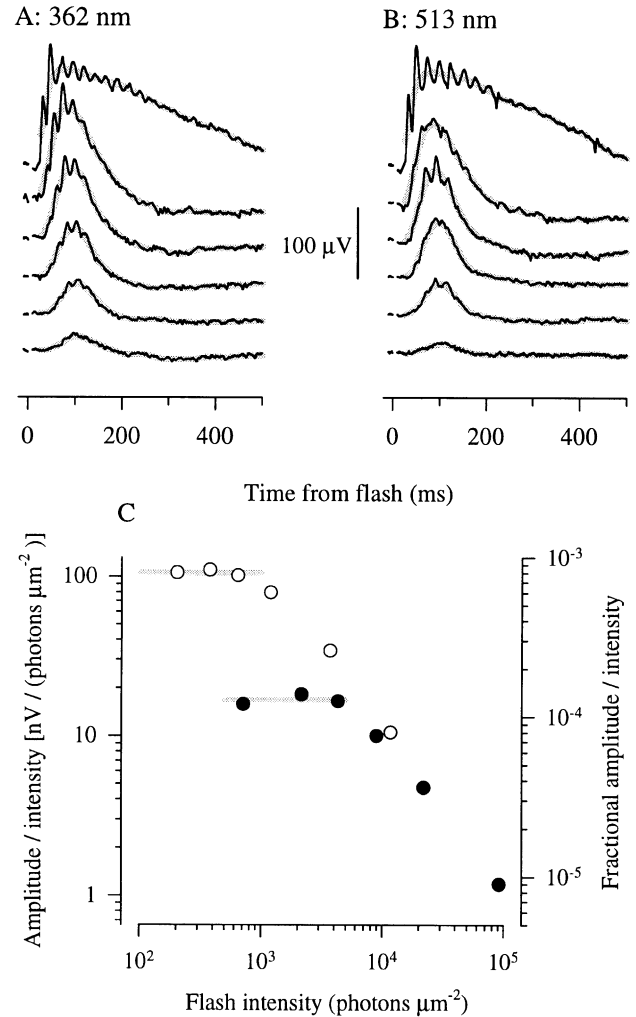


Fig. 3. Determination of the sensitivity of the cone-driven b-wave for flashes of wavelength near the  $\lambda_{\text{max}}$ 's of the two cone pigments. (A, B) Black traces show the responses of a single arrestin -/- mouse to a series of UV ( $\lambda = 362$  nm) and midwave ( $\lambda = 513$  nm) flashes: each trace is the average of from 10 to 20 individual responses. The intensities of the UV flashes (from least to most intense) were 200, 380, 640, 1200 and 3700 photons  $\mu\text{m}^{-2}$  and the midwave flash intensities were 710, 2200, 4300, 9000 and 22000 photons  $\mu\text{m}^{-2}$ , measured at the plane of the cornea. The top trace in each column is identical, and was obtained in response to a white flash estimated to isomerize 1.2% of the M-cone pigment, and 0.09% of the UV-cone pigment. The thickened gray traces were obtained by digitally filtering the averaged responses with a Gaussian function having a standard deviation  $\sigma = 12$  ms. (C) Peak amplitudes of the filtered responses of panels A, B divided by the flash intensities (left ordinate axis), or rescaled by dividing by the saturating response amplitude (right ordinate axis), plotted as a function of flash intensity; open symbols are used for responses to the 362 nm flashes, filled symbols for the responses to 513 nm flashes. The mean values of the amplitude/intensity ratio for the responses to the three least intense flashes in each response family were determined, are plotted as the gray lines. The mean values were 106 nV/(photon  $\mu\text{m}^{-2}$ ) for the responses to 362 nm flashes, and 16.9 nV/(photon  $\mu\text{m}^{-2}$ ) for the responses to the 513 nm flashes. (All rod-driven responses were suppressed by an intense flash at the beginning of the experiment, as for the arrestin -/- mouse of Fig. 1.)



maximum amplitudes of the filtered traces were measured. Panel C plots these amplitudes, divided by the flash intensity. At the lowest flash intensities, response linearity is manifested by the approximately constant value of the points, whose average is given by the gray lines. These lines thus give the *absolute sensitivity* of the cone-driven b-wave at these two wavelengths. The right-hand ordinate gives the *fractional response amplitude*, obtained by dividing the right hand ordinate scale by the saturating response amplitude ( $131 \mu\text{V}$ , or  $1.31 \times 10^5 \text{ nV}$ ); extrapolated to this ordinate, the lines yield the *fractional sensitivities* at 362 and 513 nm (see Eqs. (5)–(7)). The same analysis was repeated for the data of each animal tested, and the results are summarized in Table 1.

### 3.4. Effect of a rod-saturating background on cone-driven responses

Isolation of cone-driven responses in wild type mice requires that rod-driven activity be suppressed. One goal of this investigation was to determine the effect, if any, of a rod-saturating background on cone-driven responses. Fig. 4 presents responses obtained from a transducin  $\alpha$ -/- (upper panel) and an arrestin -/- mouse (lower panel) elicited by 362 and 513 nm flashes in the presence and absence of the standard rod-satu-

rating background (Section 2). The background caused reliable desensitization of the b-wave responses to both UV- and midwave-flashes, and shortened their time to peak (implicit time). Experiments similar to the one illustrated in Fig. 4 were performed with five transducin  $\alpha$ -/- and four arrestin -/- mice. Fig. 5 summarizes these experiments. Here the sensitivity of each group of transgenic animals relative their dark-adapted sensitivity is plotted as a function of the steady background intensity. The absolute and fractional sensitivities for all animals in the dark-adapted condition (no background), and light adapted to the standard background, are given in Table 1.

### 3.5. Recovery of cone-driven responses after intense flashes

Because the speed of recovery after intense stimuli is an important functional characteristic of cone photoreceptors, we examined the kinetics of cone b-wave recovery after intense flashes. Fig. 6 illustrates the experimental paradigm with ERGs of mice from each genotype. An achromatic conditioning flash sufficiently intense to transiently suppress all cone-driven responses was followed at different interstimulus intervals (ISIs) by a probe flash of the same intensity. In all three animals

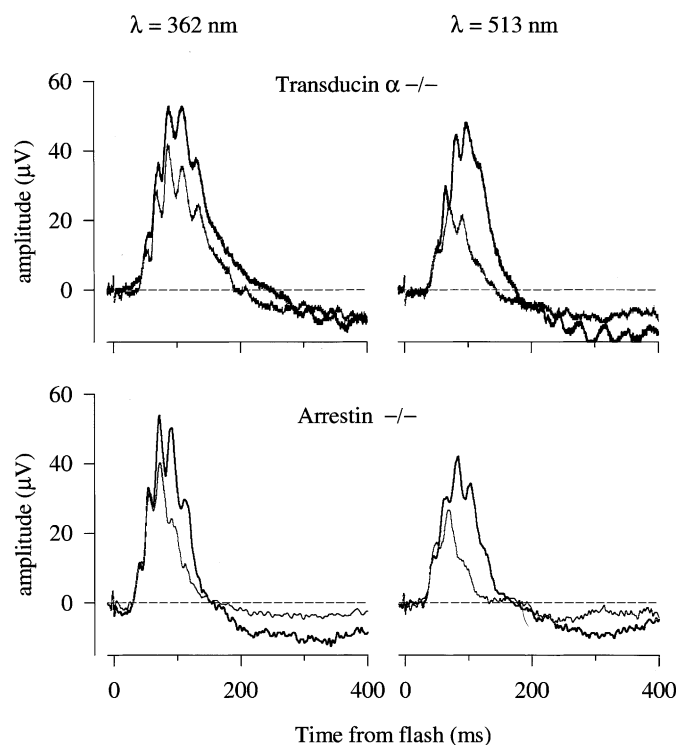


Fig. 4. Desensitizing effect of a steady background on cone b-wave sensitivity. b-wave responses for a transducin  $\alpha$ -/- and an arrestin -/- mouse in response to a 362 nm flash ( $2100 \text{ photons } \mu\text{m}^{-2}$  at the cornea) or a 513 nm flash ( $5000 \text{ photons } \mu\text{m}^{-2}$  at the cornea) were measured in darkness (black traces), or in the presence of a steady background (gray traces). The wavelength of the background was 540 nm, and its intensity was  $31\,000 \text{ photons } \mu\text{m}^{-2}$  (measured at the cornea).

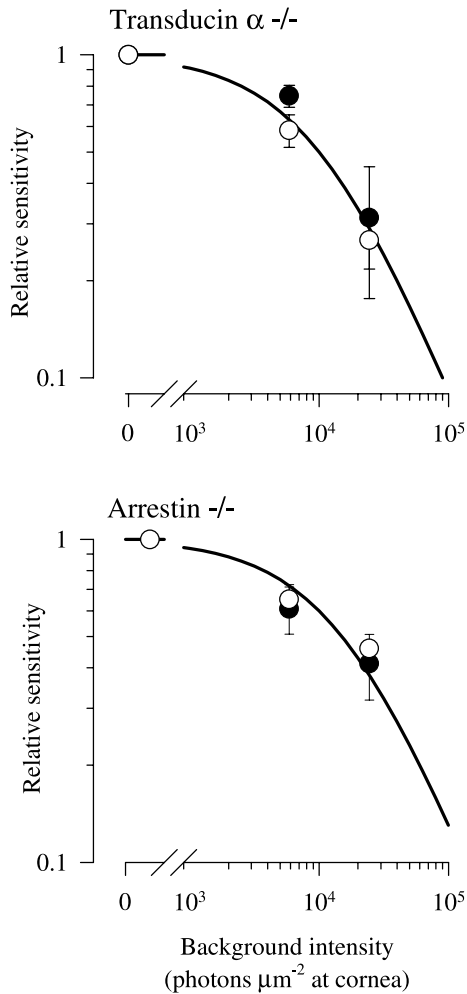


Fig. 5. Characterization of the effect of steady backgrounds on the sensitivity of the murine cone-driven b-wave. Each point is the sensitivity of 3–5 mice for 362 nm (filled circles) or 513 nm flashes (open circles), measured in the manner illustrated in Fig. 4, but normalized to the sensitivity measured in the dark; the error bars are standard deviations. The unbroken lines plot Weber's law,  $S = I_0 / (I + I_0)$ , where  $S$  is relative sensitivity,  $I$  is the background intensity and  $I_0$  is a constant, equal to 10 000 and 15 000 photons  $\mu\text{m}^{-2}$  for the data of the transducin  $\alpha^-/-$  and arrestin  $-/-$  mice, respectively.

responsivity was completely suppressed at 0.2 s after the flash, and recovery was essentially complete by 1.0 s.

Fig. 7 summarizes results obtained in the same experimental paradigm, obtained from a population of transducin  $\alpha^-/-$  mice (open symbols), arrestin  $-/-$  mice (gray symbols), and wild type mice (filled symbols). While there is considerable variation between animals, there are no systematic differences between groups. The theoretical curves shown were computed with the formulation of Smith and Lamb (1997): in panel A these curves serve as parametric “range brackets” for characterization of the entire set of results, while in panel B, the curve provides a characterization of the average recoveries. The key feature of the data can be summarized as follows: when stimulated by this intense flash, the

saturating cone b-wave amplitude recovers from 10% to 90% of its amplitude over the time window ( $t_0 - 2\tau$ ,  $t_0 + 2\tau$ ), that is, over a time window of width,  $4\tau \approx 200$  ms. Given that this flash saturates the cone a-wave (Fig. 2) and thus completely suppresses the cone circulating current, it is likely the b-wave recovery closely traces the recovery of the cone circulating current. Further evidence for this conclusion has been given in Lyubarsky et al. (2000).

#### 4. Discussion

##### 4.1. Cone a-waves in the murine ERG as a gauge of the cone circulating current

The two transgenic lines investigated are preparations in which complete isolation of cone-driven ERG responses in the mouse can be achieved. In particular, the cone a-wave can be measured with absolute confidence that rod-driven retinal activity is absent (Fig. 1). Interpreting the a-wave obtained in response to brief, intense flashes (Fig. 2) as the field potential caused by suppression of photoreceptor circulating current, the saturating magnitude of the a-wave can yield an estimate of the magnitude of the cone circulating current,  $J_{\text{circ}}$  as follows.

Specifically, based on the identification of the rod circulating current as the predominant generator of the field potential whose suppression is the dark-adapted a-wave (Section 1), the saturated amplitude of the dark-adapted a-wave can be used as a gauge for estimating the magnitudes of the generator currents of other radially oriented retinal cells. A quantitative expression for this gauge was provided by (Lyubarsky et al., 1999)

$$\frac{\Delta V_{\text{cell}}}{a_{\text{max,rods}}} = \frac{\rho_{\text{cell}}}{\rho_{\text{rods}}} \frac{J_{\text{cell}}}{J_{\text{circ,rods}}} \frac{r_{\text{cell layer}}}{r_{\text{rod layer}}}, \quad (9)$$

where  $\Delta V_{\text{cell}}$  is the electrical potential difference between corneal and reference electrodes caused by complete activation or deactivation of the generator current of particular cell type,  $\rho_{\text{cell}}$  is spatial density of the specific cell type in question in the retina,  $r_{\text{cell layer}}$  is the average resistance of the retinal layer in which the cell is found, and  $J_{\text{cell}}$  is the generator current, and  $a_{\text{max,rods}}$  is the saturated amplitude of the rod a-wave (in wild type mice). For cones  $\Delta V_{\text{cell}} = a_{\text{max,cones}}$  and  $r_{\text{cell layer}} = r_{\text{rod layer}}$ , since both rods and cones are similarly situated in the retina, and  $\rho_{\text{cones}} = 0.03\rho_{\text{rods}}$  (Carter-Dawson & LaVail, 1979a). Substituting these values into Eq. (9), and along with the specific values  $a_{\text{max,cones}} = 10 \mu\text{V}$  (Table 1) and  $a_{\text{max,rods}} = 360 \mu\text{V}$  (the value for the dark-adapted a-wave of C57/BL6 mice in Lyubarsky et al. (1999)), one obtains  $J_{\text{circ,cones}} = 0.92J_{\text{circ,rods}}$ . Further, assuming that  $J_{\text{circ,rods}} \sim 20$  pA for the murine rod

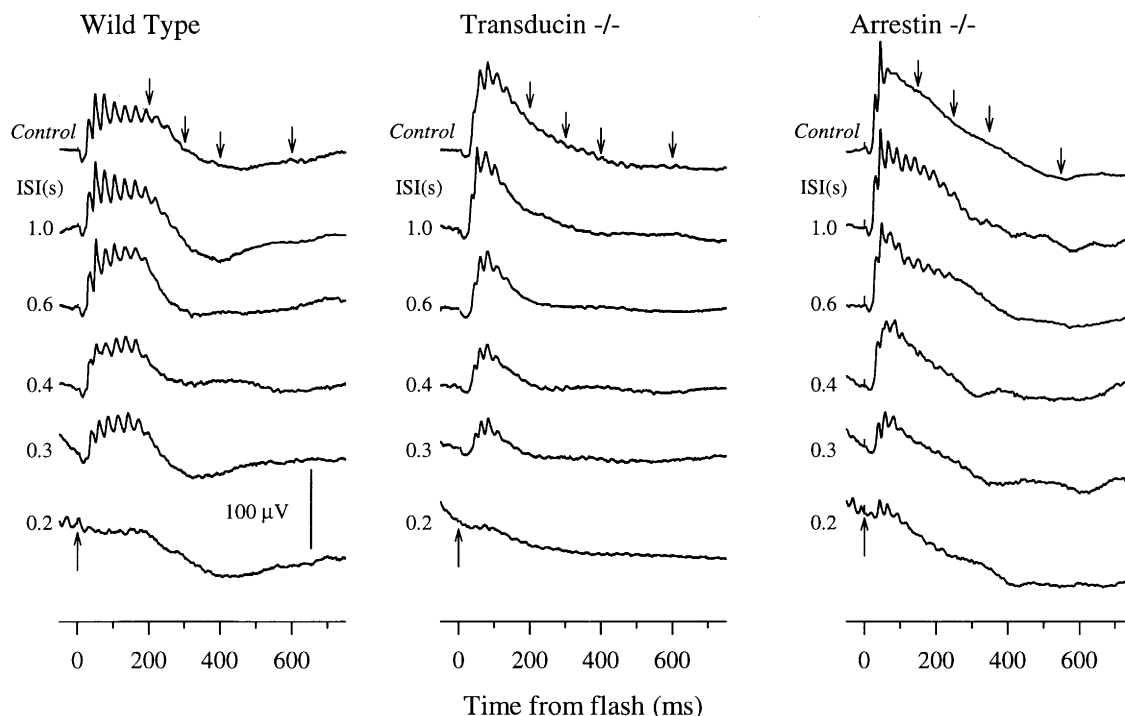


Fig. 6. Paired-flash experiment measuring the kinetics of recovery of the cone-driven ERG. An initial conditioning flash estimated to isomerize 1.2% of the M-cone pigment and 0.09% of the UV-cone pigment was delivered at  $t = 0$ ; the response to this flash in the absence of any prior stimulation is identified as “control”. At various ISIs after the initial flash, a second, identical “probe” flash was delivered. The timing of the probe flash relative to the response to the initial conditioning flash for each trace is identified by the ISI parameter nearest the curve, and (for all but the 1 s ISI) also by the down-ward pointing arrows above the “control” traces.

(Chen et al., 1999; Xu et al., 1997), we arrive at 18 pA as the estimate for the murine cone circulating current. This estimate is in reasonable agreement with published measurements from single mammalian cones, which vary from 8 to 30 pA (Kraft et al., 1990; Schnapf, Kraft, Nunn, & Baylor, 1989; Schnapf, Nunn, Meister, & Baylor, 1990).

We conclude that it is likely that the cone-driven a-waves from transducin  $\alpha$ -/- and arrestin -/- mice obtained in response to intense, brief flashes originates primarily in the suppression of cone circulating current. Additional evidence for this conclusion is provided by the kinetics and amplification of the a-wave, as described in the context of the presentation of Fig. 2. A useful practical detail of cone a-wave is its distinctive time to reach minimum (before b-wave intrusion), about 15 ms. This is a consistent feature of the ERGs of functionally rodless mice and of wild type mice whose cone a-wave is isolated with a rod-adapting background, and can be used to assess residual contribution of the rod a-wave in wild type mice, since the minimum of the rod-driven a-wave in response to intense, brief flashes is reached in less than 10 ms. A possible reason for this lengthened time to minimum is the relatively long cone membrane time constant,  $\tau_{\text{mem}} = 4\text{--}5$  ms for cones (Cideciyan & Jacobson, 1996; Schneeweis & Schnapf, 1995; Smith & Lamb, 1997).

#### 4.2. Parameters of the cone cascade estimated from the cone a-waves

In Fig. 2 we presented a formal analysis of cone a-waves of the functionally rodless mice. The analysis is complicated by the co-expression of M-pigment in the UV-cones, i.e., in cones expressing primarily the UV-pigment. We simplified this analysis by assuming the co-expression can be represented by a single proportionality constant,  $p_{M \rightarrow UV}$ . The principal conclusion is that cone a-wave data of Fig. 2 can be adequately described with an amplification constant consistent with prior values in the literature for mammalian cones,  $A = 3\text{--}7 \text{ s}^{-2}$  (Pugh & Lamb, 1993; Smith & Lamb, 1997), within the general framework presented in Section 2 for describing the population properties of murine cones.

The analysis in Fig. 2 shows that there is a tradeoff between the estimates of  $A$ , and of  $p_{M \rightarrow UV}$ , the proportion of M-pigment co-expressed in the UV-cones, such that the higher the value of  $p_{M \rightarrow UV}$ , the lower the value of  $A$  needed to fit the traces. The reason for the tradeoff between  $A$  and  $p_{M \rightarrow UV}$  is that the higher is the proportion of co-expressed M-pigment, the larger the quantity of the M-pigment isomerized in the UV-cones by the white flashes (Eq. (2)). Because the UV-cones will experience a higher total number  $\Phi$  of photoisomerizations

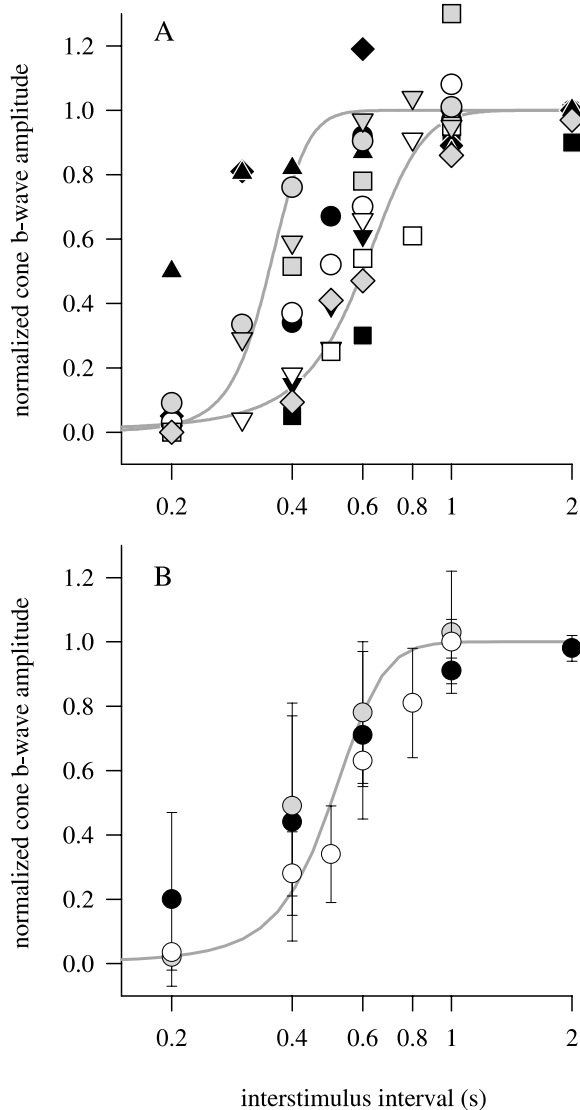


Fig. 7. Time course of recovery of cone-driven b-wave responses for wild type (black symbols) transducin  $\alpha^{-/-}$  (white symbols) and arrestin  $-/-$  (gray symbols) from an intense conditioning flash, plotted as a function of the ISI, i.e., the time between the conditioning and probe flashes. The experimental paradigm is illustrated in Fig. 6. (A) Data of individual mice. The amplitudes were measured from Gaussian-filtered traces (see Fig. 3), and are normalized by the amplitude of the response, measured after at least 3 s. The smooth traces we computed with the formula of Thomas and Lamb (1999) used to describe rod a-wave recovery, amplitude  $(t) = 1/[1 + \exp(-(t - t_0)/\tau)]$ . The two curves, which have the parameter values  $t_0 = 0.35$  s and  $\tau = 0.04$  s (left curve), and  $t_0 = 0.6$  s and  $\tau = 0.11$  s (right curve), are seen to bracket most of the data points. (B) Average recovery time course. Points and error bars plot the mean  $\pm$  s.d. of the data in panel A, at i.s.i. values for which at least measurements for at least three animals were available. The smooth curve has the same formulation as the curves in panel A, with values  $t_0 = 0.5$  s and  $\tau = 0.05$  s.

from a given white flash as the proportion of co-expressed M-pigment rises, a smaller value of  $A$  will suffice to achieve the observed a-wave activation rate (see Eq. (3)). Based on previous estimates of  $A$  for mammalian cones,  $A = 3\text{--}7$  s $^{-2}$ , it is unlikely that  $A$  for cones ex-

ceeds 10, and so we conclude that  $p_{M \rightarrow UV}$  likely exceeds 5% on average. However, a co-expression proportion  $p_{M \rightarrow UV}$  as high as 0.2 is also consistent with the model analysis of the cone a-wave data (Fig. 2, panels D, F).

#### 4.3. Cone-driven b-waves in ERGs of the functionally rodless mice: amplitude and sensitivity

Both transducin  $\alpha^{-/-}$  and arrestin  $-/-$  mice generate cone-driven, corneal-positive (b-wave) responses very similar to ERGs recorded from wild type animals (Fig. 1; Lyubarsky et al., 1999). The saturating amplitudes, absolute sensitivities, and spectral sensitivities of the b-waves for these transgenic animals are statistically indistinguishable from those of wild type mice (Table 1). From this it can be concluded that these functionally rodless mice have a normal density of both the UV- and M-type cones, and normal cone on-bipolar density (interpreting the b-wave as a field potential originating primarily in cone on-bipolars).

#### 4.4. Cone b-wave threshold and assessment of rod function from the b-wave

An important quantity that can be derived from the absolute sensitivity of the cone b-waves of the functionally rodless mice is the cone b-wave ‘‘threshold’’, i.e., the flash intensity required to get a reliable cone-driven response in a dark-adapted mouse. This quantity is important because it can serve as a benchmark for determining whether rod function is present, for example, in mice that are undergoing rod degeneration: thus, it cannot be unequivocally concluded that rod function is present from the b-wave unless the responses are recorded in response to flashes whose intensities are well below the cone threshold.

Keeping in mind that the threshold amplitude requires selection of a somewhat arbitrary criterion, we will adopt a threshold amplitude criterion of 10  $\mu$ V. Then, based on an absolute sensitivity of about 10 nV/(photon  $\mu$ m $^{-2}$ ) for 513 nm light (Table 1, row 4, no background condition), a 10  $\mu$ V M-cone-driven b-wave response would be achieved with a flash intensity of 1000 photons  $\mu$ m $^{-2}$  at the cornea (see Fig. 3(B,C)). This latter intensity corresponds to a Ganzfeld luminance of about 0.2 scotopic cd s m $^{-2}$  (Eq. (1)), and in mice with normal rods will generate about 200 photoisomerizations rod $^{-1}$  (Lyubarsky & Pugh, 1996).

Toda, Bush, Humphries, and Sieving (1999) reported the b-wave threshold (5  $\mu$ V criterion) for young rhodopsin  $-/-$  mice to be 0.09 photopic cd s m $^{-2}$ ; these mice, like the two strains investigated here, are a model system for investigation of murine cone-driven retinal function. When adjustments are made for the 2-fold lower amplitude criterion and for the conversion from photopic to scotopic units (1.4), the estimated cone

threshold for rhodopsin  $-/-$  mice for a 10  $\mu\text{V}$  criterion is found to be  $0.09 \times 2 \times 1.4 = 0.25$  scotopic  $\text{cd s m}^{-2}$ , within error of the value, 0.2 scotopic  $\text{cd s m}^{-2}$ , just estimated for transducin  $\alpha-/-$  and arrestin  $-/-$  mice.<sup>2</sup>

One cannot conclude unequivocally, then, that a b-wave response whose amplitude is 10  $\mu\text{V}$  or less in response to a flash whose intensity is at or higher than the calculated threshold intensity,  $\approx 0.2$  scotopic  $\text{cd s m}^{-2}$ , has its origin in rod-driven neurons. Stated more generally, b-wave responses with flash sensitivity less than about 50 nV per scotopic  $\text{cd s m}^{-2}$  cannot be securely assigned to rod-driven neurons. This cautionary point applies particularly to ERGs obtained from mice with lower than normal rod density (such as is usually the case in retinal degeneration), or to ERGs of mice whose rods are missing components of the phototransduction cascade, since it can be anticipated that the responsivity of rod-driven responses in these cases will be depressed. In summary, no claim to have preserved or therapeutically restored rod function can be made unequivocally on the basis of b-wave responses obtained with flashes of intensity exceeding the cone b-wave threshold. In addition, claims of rod function based on a-waves require that the a-wave magnitude materially exceed the saturated cone a-wave amplitude, about 10  $\mu\text{V}$ .

#### 4.5. Midwave background desensitization of UV flash responses: a further corroboration of cone-pigment co-expression

It has been observed that all cone-driven ERG activity in mice can be transiently suppressed by an intense “orange” conditioning flash, and concluded that this phenomenon could only be explained if cones expressing primarily the UV-cone pigment also co-expressed the M-pigment (Lyubarsky et al., 1999). A recent immunohistochemical investigation (Applebury et al., 2000) has substantiated previous evidence for cone pigment co-expression in mice (Gloesman & Ahnelt, 1998; Rohlich et al., 1994), and provided evidence that co-expression extends to virtually all the cones in the retina (while varying in degree with the retinal location).

The results presented here provide further evidence for cone pigment co-expression in mice. Specifically, as seen in here in Figs. 4 and 5, the standard rod-saturating background of 540 nm desensitized the cone b-wave responses not only to 513 nm flashes, but also to 362 nm flashes. The desensitization of the responses to 362 nm flashes cannot be attributed to absorption of the 540 nm light by the UV-cone pigment. To arrive at this conclusion, we employed the template developed by

(Lamb, 1995), which describes the absorbance spectra of a large family of photopigments over  $7 \log_{10}$  units of sensitivity on the long wavelength side of the spectrum. The computed absorbance at 540 nm for a pigment with  $\lambda_{\text{max}} = 360$  nm is less than  $10^{-5}$  of the maximum. Assuming the end-on collecting area for the UV-cones of a mouse in a ganzfeld (expressed in terms of light measured at the cornea) is 0.14  $\mu\text{m}^2$  at the  $\lambda_{\text{max}}$  (Lyubarsky et al., 2000), we thus estimate the collecting area at the cornea for 540 nm of a cone expressing only a 360 nm pigment to be  $\approx 1.4 \times 10^{-6}$   $\mu\text{m}^2$ , 100 000-fold reduced from the  $\lambda_{\text{max}}$ . For our standard rod-suppressing background, which delivers 31 000 photons $^{-1}$  s $^{-1}$   $\mu\text{m}^{-2}$  at the cornea, the estimated rate of photoisomerizations for such a cone is thus  $31\,000 \times 1.4 \times 10^{-6} = 0.043$  photoisomerizations s $^{-1}$ . This is equivalent to 1 photoisomerization per cone every 23 s. Because mammalian cones require many hundreds to thousands of photoisomerizations s $^{-1}$  to become desensitized (Baylor, Nunn, & Schnapf, 1984; Schnapf et al., 1989, 1990), photons captured by the UV-cone pigment from the 540 nm background could not cause the desensitization seen in Figs. 4 and 5. An alternative hypothesis to co-expression is that of convergence of signals from UV- and M-cones onto the same bipolar cells. We deem this unlikely, since histological evidence indicates that cones expressing predominantly one or the other pigment are not found in the same retinotopic location (Applebury et al., 2000; Rohlich et al., 1994; Szel, Rohlich, Caffè, & van Veen, 1996).

#### 4.6. Utility of functionally rodless mice in the investigation of retinal disease and in gene therapy

We conclude by commenting that the transgenic lines of mice investigated here may have considerable utility in the investigation of the progression of disease originating in rods, and in therapeutic interventions in such disease progression. Thus, in both lines of mice investigated here, one can readily probe the functional status of cones, and determine when and to what extent cone-driven retinal function has been compromised by manipulations such as introduction of a rod-specific transgene that causes rod degeneration, or alternatively, protected from decline by a therapeutic intervention such as gene restoration by a viral vector. Another line of transgenic mice that shows promise for characterizing cone function is rhodopsin  $-/-$  mouse, recently developed in two laboratories (Humphries et al., 1997; Lem et al., 1999). However, while the necessarily cone-driven ERGs of *young* rhodopsin  $-/-$  mice are similar in all reported respects to those described here for transducin  $\alpha-/-$  and arrestin  $-/-$  mice, there is a fundamental difference: rhodopsin  $-/-$  mice do not have a stationary night blindness. Rather, at about 50 days the latter undergo a rapid retinal degeneration (Toda et al., 1999).

<sup>2</sup> Neither human scotopic or photopic units are ideal for describing stimulation of murine cones, given the cones pigment  $\lambda_{\text{max}}$ 's, 359 and 508 nm. However, since the M-cone  $\lambda_{\text{max}}$  is close to that of rhodopsin, use of scotopic photometric units is not unreasonable.

Arrestin  $-/-$  have already been shown to have an increased susceptibility (relative to wild type) for light-induced damage (Chen et al., 1999), and thus could serve as a model for the progression of cone degeneration following light-induced damage to rods. Transducin  $\alpha-/-$  mice afford the important opportunity of determining to what extent light or other rod-dependent retinal damage is independent of the rod cascade activity subsequent to the activation of rhodopsin, since these animals' rods have no G-protein activation, PDE activation, or electrical response (Calvert et al., 2000). Since transducin  $\alpha-/-$  retinas nonetheless do undergo light-dependent damage (Lem, unpublished observations), cone function in these animals could be probed under conditions of retinal deterioration, and strategies for preservation of cone function tested.

### Acknowledgements

Supported by funds from the NIH and the Research to Prevent Blindness Foundation.

### References

- Applebury, M. L., Antoch, M. P., Baxter, L. C., Chun, L. L., Falk, J. D., Farhangfar, F., Kage, K., Krzystolik, M. G., Lyass, L. A., & Robbins, J. T. (2000). The murine cone photoreceptor: a single cone type expresses both S and M opsins with retinal spatial patterning. *Neuron*, *27*, 513–523.
- Baylor, D. A., Nunn, B. J., & Schnapf, J. L. (1984). The photocurrent, noise and spectral sensitivity of rods of the monkey *Macaca fascicularis*. *Journal of Physiology*, *357*, 575–607.
- Biel, M., Seeliger, M., Pfeifer, A., Kohler, K., Gerstner, A., Ludwig, A., Jaissle, G., Fauser, S., Zrenner, E., & Hofmann, F. (1999). Selective loss of cone function in mice lacking the cyclic nucleotide-gated channel CNG3. *Proceedings of the National Academy of Sciences of the United States of America*, *96*, 7553–7557.
- Calvert, P. D., Krasnoperova, N. V., Lyubarsky, A. L., Isayama, T., Nicolo, M., Kosaras, B., Wong, G., Gannon, K. S., Margolskee, R. F., Sidman, R. L., Pugh, E. N., Jr., Makino, C. L., & Lem, J. (2000). Phototransduction in transgenic mice after targeted deletion of the rod transducin alpha-subunit. *Proceedings of the National Academy of Sciences of the United States of America*, *97*, 13913–13918.
- Carter-Dawson, L. D., & LaVail, M. M. (1979a). Rods and cones in the mouse retina. I. Structural analysis using light and electron microscopy. *Journal of Comparative Neurology*, *188*, 245–262.
- Carter-Dawson, L. D., & LaVail, M. M. (1979b). Rods and cones in the mouse retina. II. Autoradiographic analysis of cell generation using tritiated thymidine. *Journal of Comparative Neurology*, *188*, 263–272.
- Chen, J., Simon, M. I., Matthes, M. T., Yasumura, D., & LaVail, M. M. (1999). Increased susceptibility to light damage in an arrestin knockout mouse model of Oguchi disease (stationary night blindness). *Investigative Ophthalmology & Visual Science*, *40*, 2978–2982.
- Cideciyan, A. V., & Jacobson, S. G. (1996). An alternative phototransduction model for human rod and cone ERG a-waves: normal parameters and variation with age. *Vision Research*, *36*, 2609–2621.
- Gloesman, M., & Ahnelt, P. K. (1998). Coexpression of M- and S-opsin extends over entire inferior mouse retina. *Investigative Ophthalmology & Visual Science*, *39*, S1059.
- Green, D. G., & Kapousta-Bruneau, N. V. (1999). A dissection of the electroretinogram from the isolated rat retina with microelectrodes and drugs. *Visual Neuroscience*, *16*, 727–741.
- Hetling, J. R., & Pepperberg, D. R. (1999). Sensitivity and kinetics of mouse rod flash responses determined in vivo from paired-flash electroretinograms. *Journal of Physiology*, *516*, 593–609.
- Humphries, M. M., Rancourt, D., Farrar, G. J., Kenna, P., Hazel, M., Bush, R. A., Sieving, P. A., Sheils, D. M., McNally, N., Creighton, P., Erven, A., Boros, A., Gulya, K., Capecchi, M. R., & Humphries, P. (1997). Retinopathy induced in mice by targeted disruption of the rhodopsin gene. *Nature Genetics*, *15*, 216–219.
- Kraft, T. W., Makino, C. L., Mathies, R. A., Lugtenburg, J., Schnapf, J. L., & Baylor, D. A. (1990). Cone excitations and color vision. *Cold Spring Harbor Symposia on Quantitative Biology*, *55*, 635–641.
- Lamb, T. D. (1995). Photoreceptor spectral sensitivities: common shape in the long-wavelength region. *Vision Research*, *35*, 3083–3091.
- Lamb, T. D., & Pugh, E. N., Jr. (1992). A quantitative account of the activation steps involved in phototransduction in amphibian photoreceptors. *Journal of Physiology*, *449*, 719–758.
- Lem, J., Krasnoperova, N. V., Calvert, P. D., Kosaras, B., Cameron, D. A., Nicolo, M., Makino, C. L., & Sidman, R. L. (1999). Morphological, physiological, and biochemical changes in rhodopsin knockout mice. *Proceedings of the National Academy of Sciences of the United States of America*, *96*, 736–741.
- Leskov, I. B., Klenchin, V. A., Handy, J. W., Whitlock, G. G., Govardovskii, V. I., Bownds, M. D., Lamb, T. D., Pugh, E. N., Jr., & Arshavsky, V. Y. (2000). The gain of rod phototransduction: reconciliation of biochemical and electrophysiological measurements. *Neuron*, *27*, 525–537.
- Lyubarsky, A. L., Chen, C. K., Simon, M. I., & Pugh, E. N., Jr. (2000). Mice lacking G-protein receptor kinase 1 have profoundly slowed recovery of cone-driven retinal responses. *Journal of Neuroscience*, *20*, 2209–2217.
- Lyubarsky, A. L., Falsini, B., Pennesi, M. E., Valentini, P., & Pugh, E. N., Jr. (1999). UV- and midwave-sensitive cone-driven retinal responses of the mouse: a possible phenotype for coexpression of cone photopigments. *Journal of Neuroscience*, *19*, 442–455.
- Lyubarsky, A. L., & Pugh, E. N., Jr. (1996). Recovery phase of the murine rod photoresponse reconstructed from electroretinographic recordings. *Journal of Neuroscience*, *16*, 563–571.
- Nakatani, K., Tamura, T., & Yau, K. W. (1991). Light adaptation in retinal rods of the rabbit and two other nonprimate mammals. *Journal of General Physiology*, *97*, 413–435.
- Penn, R. D., & Hagins, W. A. (1972). Kinetics of the photocurrent of retinal rods. *Biophysical Journal*, *10*, 380–412.
- Pennesi, M. E., Lyubarsky, A. L., & Pugh, E. N., Jr. (1998). Extreme responsiveness of the pupil of the dark-adapted mouse to steady retinal illumination. *Investigative Ophthalmology & Visual Science*, *39*, 2148–2156.
- Pugh, E. N., Jr., Falsini, B., & Lyubarsky, A. L. (1998). The origin of the major rod- and cone-driven components of the rodent electroretinogram and the effect of age and light-rearing history on the magnitude of these components. In T. Williams, & A. Thistle (Eds.), *Photostasis and Related Phenomena* (pp. 93–128). New York: Plenum Press.
- Pugh, E. N., Jr., & Lamb, T. D. (1993). Amplification and kinetics of the activation steps in phototransduction. *Biochimica et Biophysica Acta*, *1141*, 111–149.
- Robson, J. G., & Frishman, L. J. (1995). Response linearity and kinetics of the cat retina: the bipolar cell component of the dark-adapted electroretinogram. *Visual Neuroscience*, *12*, 837–850.
- Robson, J. G., & Frishman, L. J. (1996). Photoreceptor and bipolar cell contributions to the cat electroretinogram: a kinetic model for

- the early part of the flash response. *Journal of the Optical Society of America A*, *13*, 613–622.
- Rohlich, P., van Veen, T., & Szel, A. (1994). Two different visual pigments in one retinal cone cell. *Neuron*, *13*, 1159–1166.
- Schnapf, J. L., Kraft, T. W., Nunn, B. J., & Baylor, D. A. (1989). Transduction in primate cones. *Neuroscience Research Supplement*, *10*, S9–S14.
- Schnapf, J. L., Nunn, B. J., Meister, M., & Baylor, D. A. (1990). Visual transduction in cones of the monkey *Macaca fascicularis*. *Journal of Physiology*, *427*, 681–713.
- Schneeweis, D., & Schnapf, J. L. (1995). Photovoltage of rods and cones in the macaque retina. *Science*, *268*, 1053–1056.
- Smith, N. P., & Lamb, T. D. (1997). The a-wave of the human electroretinogram recorded with a minimally invasive technique. *Vision Research*, *37*, 2943–2952.
- Sun, H., Macke, J. P., & Nathans, J. (1997). Mechanisms of spectral tuning in the mouse green cone pigment. *Proceedings of the National Academy of Sciences of the United States of America*, *94*, 8860–8865.
- Szel, A., Rohlich, P., Caffè, A. R., & van Veen, T. (1996). Distribution of cone photoreceptors in the mammalian retina. *Microscopy Research and Technique*, *35*, 445–462.
- Tamura, T., Nakatani, K., & Yau, K.-W. (1991). Calcium feedback and sensitivity regulation in primate rods. *Journal of General Physiology*, *98*, 95–130.
- Thomas, M. M., & Lamb, T. D. (1999). Light adaptation and dark adaptation of human rod photoreceptors measured from the a-wave of the electroretinogram. *Journal of Physiology*, *518*, 479–496.
- Toda, K., Bush, R. A., Humphries, P., & Sieving, P. A. (1999). The electroretinogram of the rhodopsin knockout mouse. *Visual Neuroscience*, *16*, 391–398.
- Wyszecki, G., & Stiles, W. S. (1982). *Color Science*. New York: Wiley.
- Xu, J., Dodd, R. L., Makino, C. L., Simon, M. I., Baylor, D. A., & Chen, J. (1997). Prolonged photoresponses in transgenic mouse rods lacking arrestin. *Nature*, *389*, 505–509.
- Yokoyama, S., Radlwimmer, F. B., & Kawamura, S. (1998). Regeneration of ultraviolet pigments of vertebrates. *FEBS Letters*, *423*, 155–158.